MR-3993

AD-A254 713

MEMORANDUM REPORT BRL-MR-3993

BRL

A MODEL FOR FULLY FORMED SHEAR BANDS

T. W. WRIGHT
U.S. ARMY BALLISTIC RESEARCH LABORATORY

H. OCKENDON
UNIVERSITY OF OXFORD

AUGUST 1992

U.S. ARMY LABORATORY COMMAND

BALLISTIC RESEARCH LABORATORY
ABERDEEN PROVING GROUND, MARYLAND

NOTICES

Destroy this report when it is no longer needed. DO NOT return it to the originator.

Additional copies of this report may be obtained from the National Technical Information Service, U.S. Department of Commerce, 5285 Port Royal Road, Springfield, VA 22161.

The findings of this report are not to be construed as an official Department of the Army position, unless so designated by other authorized documents.

The use of trade names or manufacturers' names in this report does not constitute indorsement of any commercial product.

REPORT DOCUMENTATION PAGE

Form Approved
OMB No. 0704-0188

1. AGENCY USE ONLY *(Leave blank)*

2. REPORT DATE
August 1992

3. REPORT TYPE AND DATES COVERED
Final, Jan 91–Dec 91

4. TITLE AND SUBTITLE
A Model for Fully Formed Shear Bands

5. FUNDING NUMBERS
PR: IL161102AH43

6. AUTHOR(S)
T. W. Wright and H. Ockendon*

7. PERFORMING ORGANIZATION NAME(S) AND ADDRESS(ES)

8. PERFORMING ORGANIZATION REPORT NUMBER

9. SPONSORING/MONITORING AGENCY NAME(S) AND ADDRESS(ES)
U.S. Army Ballistic Research Laboratory
ATTN: SLCBR-DD-T
Aberdeen Proving Ground, MD 21005-5066

10. SPONSORING/MONITORING AGENCY REPORT NUMBER
BRL-MR-3993

11. SUPPLEMENTARY NOTES
* Mathematical Institute, University of Oxford, Oxford, England

12a. DISTRIBUTION / AVAILABILITY STATEMENT
Approved for public release; distribution is unlimited.

12b. DISTRIBUTION CODE

13. ABSTRACT *(Maximum 200 words)*

An asymptotic analysis of the morphology of a fully formed shear band is given for a simple flow law in a perfectly plastic material. Scaling laws are given for the maximum strain rate and the width of the band.

14. SUBJECT TERMS
plastic flow; plastic deformation; adiabatic shear banding

15. NUMBER OF PAGES
31

16. PRICE CODE

17. SECURITY CLASSIFICATION OF REPORT	18. SECURITY CLASSIFICATION OF THIS PAGE	19. SECURITY CLASSIFICATION OF ABSTRACT	20. LIMITATION OF ABSTRACT
UNCLASSIFIED	UNCLASSIFIED	UNCLASSIFIED	SAR

INTENTIONALLY LEFT BLANK.

TABLE OF CONTENTS

INTENTIONALLY LEFT BLANK.

1. INTRODUCTION

Adiabatic shear bands form in a deforming material when thermal softening, due to plastic heating, is stronger than work hardening and rate hardening combined, so that a regime with net strain softening occurs. Numerical studies by Walter (1992) have shown that, after a period of relatively slow growth of perturbations, it often happens that an extreme localization of the deformation occurs suddenly so that subsequent deformation is confined almost entirely to a narrow strip or band of material, which becomes very hot relative to the adjacent, almost nondeforming material. Within these narrow bands, often measured in a few tens of microns or less, heat production from plastic working is nearly balanced by heat conduction down extremely steep temperature gradients.

In studies on adiabatic shear bands (the name is an historical misnomer), a recurring question is the "width" of the band, which should be definitively furnished by the theory. It is the purpose of this report to answer that question, at least within the context of a simple model, by examining the morphology of a fully formed band in the late stages of deformation.

2. THE MODEL

Wright and Walter (1987) used the following dimensional equations as a prototypical model for adiabatic shear banding:

$$s_y = \rho v_t \tag{1.1}$$

$$s_t = \mu(v_y - \dot{\gamma}_p) \tag{1.2}$$

$$\rho c \vartheta_t = k \vartheta_{yy} + s\dot{\gamma}_p \tag{1.3}$$

$$s = \kappa_0 (1 - a\vartheta)(1 + b\dot{\gamma}_p)^m \,. \tag{1.4}$$

Boundaries at $y = \pm h$ are assumed to be moving at constant velocity and to be fully insulated. The spatial coordinate perpendicular to the slab is y, time is t, and subscripts in y or t indicate partial derivatives. Equation 1.1 represents balance of linear momentum in a one-dimensional slab of incompressible material undergoing simple shearing, where s is shear stress, v is particle velocity in the plane of the slab, and ρ is density. Equation 1.2 gives the conventional, additive decomposition of elastic and plastic strain rates, where ρ is the elastic shear modulus, v_y is the total shear strain rate, and $\dot{\gamma}_p$ is the plastic strain rate. Equation 1.3 represents balance of energy, where ϑ is temperature (measured from an arbitrary reference level), and c and k are physical constants for heat capacity and thermal conductivity, respectively. It has been tacitly assumed that thermal and mechanical influences are totally uncoupled in the internai energy of the material, that the dependence of internal energy on temperature is only linear, and furthermore, that all the plastic work is converted instantaneously into heat. Equation 1.4 is the assumed flow law for an elastic, perfectly plastic material with thermal softening and rate hardening, where κ_0, a, b, and m are physical constants. In metals, the strain rate sensitivity is very small, $m < .03$ in most cases. In actual practice, the flow law is used as a definition for $\dot{\gamma}_p$ when $s > \kappa_0 (1 - a\vartheta)$; otherwise, $\dot{\gamma}_p \equiv 0$. In this simple model, work hardening has been ignored; in a more realistic model, an evolutionary law would have to be specified for the strength κ_0.

A numerical study by Walter (1992), which as far as the authors are aware, contains the only extensive treatment of fully formed shear bands, has shown that the model may be further simplified without significant loss of realism in certain circumstances. Thus, if the density times the square of the imposed boundary velocity and divided by a characteristic stress is small compared to 1 ($\rho v_0^2/S_0 \ll 1$), then the stress stays essentially independent of y even though it may change extremely rapidly with time. If the shear modulus is large compared to a characteristic stress ($\mu/S_0 \gg 1$), as is generally true for metals, then after some initial transients, the plastic strain rate and the total strain rate become nearly identical. Finally, since $b\dot{\gamma}_p \gg 1$ in most of the deformation, the flow law may be simplified accordingly. When these simplifications are taken into account, and the following scheme of nondimensionalization has been used

$$
\begin{aligned}
&\bar{y} = y/h, && \bar{t} = \dot{\gamma}_0 t && \\
&\bar{s} = s/S_0, && \bar{\vartheta} = \rho c \vartheta/S_0, && \bar{v} = v/\dot{\gamma}_0 h \\
&\bar{\rho} = \rho\,(\dot{\gamma}_0 h)^2/S_0, && \bar{k} = k/\rho c \dot{\gamma}_0 h^2, && \bar{a} = aS_0/\rho c
\end{aligned}
\qquad (2)
$$

then a reduced set of equations, now in nondimensional form, but with the bars dropped for clarity, is as follows:

$$s_y = 0 \tag{3.1}$$

$$\vartheta_t = k\vartheta_{yy} + sv_y \tag{3.2}$$

$$s = (1 - a\vartheta)v_y^m \tag{3.3}$$

The nominal applied strain rate is $\dot{\gamma}_0$, so the velocity maintained on the boundary is $v_0 \equiv \dot{\gamma}_0 h$, and $S_0 \equiv \kappa_0 (b\dot{\gamma}_0)^m$ is a characteristic stress. Boundary conditions for the reduced problem are taken to be $v(\pm 1, t) = \pm 1$ and $\vartheta_y(\pm 1, t) = 0$. For convenience, only symmetrical solutions will be considered further (i.e., $v(0, t) = 0$, $v(1, t) = 1$, $\vartheta_y(0, t) = \vartheta_y(1, t) = 0$).

3. A NONLINEAR EIGENVALUE PROBLEM

In their 1987 paper, Wright and Walter noticed that in their numerical solutions the strain rate became essentially independent of time in the late stages of deformation, although the temperature and stress continued to evolve. Accordingly, they proposed a set of equations to describe the terminal behavior (which they termed quasi-steady) but they did not analyse those equations further. An equivalent set of equations follows.

First, define a new dependent variable, $u(y)$, from $v_y = Au^{-1/m}$, where A is the constant strain rate in the center of the band, and u does not depend on time. From the flow law (Equation 3.3), $u = A^m(1 - a\vartheta)/s$, and from Equation 3.1 and Equation 3.2, u satisfies

$$k\frac{u_{yy}}{u} - a\,A^{1+m}\,u^{-(1+m)/m} = \frac{\dot{s}}{s} = -\alpha\,. \tag{4}$$

Since it has been assumed that u depends only on y, and s only on t, it follows by the usual separation argument that α is a constant. Thus, an observation about numerical results has led to a pair of ordinary differential equations,

$$u_{yy} + \frac{\alpha}{k}u - \frac{a}{k}A^{1+m}u^{-1/m} = 0, \quad \dot{s} + \alpha s = 0, \tag{5}$$

the solution of which will be a special solution of the partial differential equations (Equations 3.1, 3.2, and 3.3). The eigenvalue, α, and the normalizing constant, A, must be determined as part of the solution.

From the definition of u, we have $u(0) = 1$, and from the boundary conditions on ϑ, we have $u_y(0) = u_y(1) = 0$. Because of the boundary conditions on v, the integral of the strain rate,

$$\int_0^1 v_y dy = 1,$$

implies

$$\int_0^1 u^{-1/m} dy = A^{-1}.$$

Then integration of Equation 5, together with the use of this result and the boundary conditions on u, implies

$$\int_0^1 u dy = aA^m/\alpha. \tag{6}$$

A first integral of Equation 5 that satisfies boundary conditions at y = 0 is

$$u_y^2 = \lambda(1 - u^{-p}) - \nu(u^2 - 1) \tag{7}$$

where the constants λ, p, and ν are given by

$$\lambda = \frac{2am}{k(1 - m)}A^{1+m}, \tag{8.1}$$

$$p = \frac{1 - m}{m}, \tag{8.2}$$

$$v = \frac{\alpha}{k}. \tag{8.3}$$

Since p is large ($p > 30$ for metals), the phase portrait corresponding to Equation 7 looks nearly circular in coordinates u_y vs. $\sqrt{vu}$ until u gets close to 1, and then it drops sharply back to 0, as shown in Figure 1. The radius of the circle is nearly $\sqrt{\lambda + v}$, as shown. The curve is parameterized by the y-coordinate with the boundaries $y = 0$ and $y = 1$ lying at the intersections where $u' = 0$. Although the interval $0 \le y \le 1$ may correspond to multiple circuits around the phase diagram, from now on attention will be focused only on a half circuit with $u(0) = 1$ and $u(1) = \sqrt{1 + \lambda/v}$, which corresponds to the sketches for u and v_y, as shown in Figure 1. Sketches of solutions corresponding to multiple circuits may be obtained by obvious reflections and periodic extensions. It should be noted as well that since $a\vartheta = 1 - sA^{-m}u$, the temperature distribution will look like u, only linearly scaled and turned upside down. The important point to note is that the temperature distribution will appear to be much broader than the strain rate distribution, which will be intensely concentrated near the origin due to the smallness of the parameter m.

Figure 1 suggests that inner and outer approximations to the solution should be sought corresponding to the left and right sides of the phase portrait. In the outer solution, $u > 1$ and $u^{-p} \ll 1$, and so we write

$$(u'_0)^2 = \lambda + v - vu_0^2 \tag{9}$$

with boundary condition $u'_0(1) = 0$. In Equation 9, at this stage the relative size of λ and v is unknown. The solution that matches the boundary condition at $y = 1$ is

$$u_0 = \sqrt{1 + \frac{\lambda}{v}} \cos\sqrt{v}\,(1 - y). \tag{10}$$

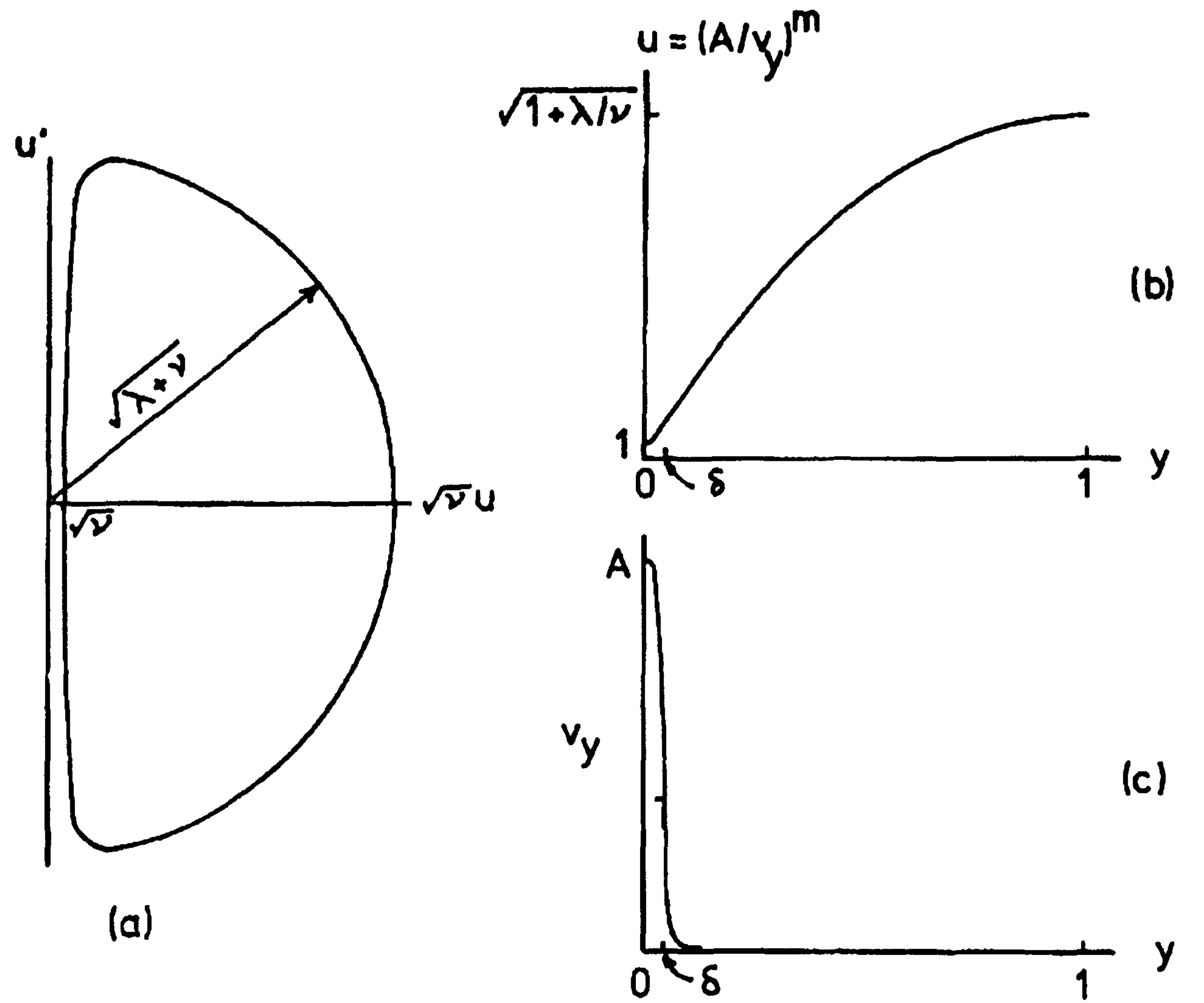

Figure 1. (a) Sketch of Phase Portrait, Equation 7, (b) Sketch of Solution u(y), or Inverted Sketch of ϑ (y), (c) Sketch of Strain Rate $\dot{\gamma} = v_y(y)$.

We note that $u_0 \to \sqrt{1 + \frac{\lambda}{v}} \cos\sqrt{v} + \sqrt{\lambda + v}\ y \sin\sqrt{v} + 0(y^2)$ as $y \to 0$.

For the inner solution, u is near to 1. We write $u_i = 1 + q$, and since $u_i^{-p} \approx e^{-pq}$ for $q \ll 1$, q should satisfy

$$(q')^2 = \lambda(1 - e^{-pq}) - v(2q + q^2) \tag{11}$$

As q approaches 0, the right-hand side of Equation 11 approaches $(\lambda p - 2v)q$. Since p is large compared to 1, even if v and λ are comparable in size, it still turns out that $2v \ll \lambda p$, so the second term on the right-hand side of Equation 11 may be dropped for now, subject to verification of orders of magnitude later. Putting $r = e^{-pq}$, by quadrature we find the solution to Equation 11 to be $r = \operatorname{sech}^2\left(\frac{1}{2}p\sqrt{\lambda}y\right)$, or in the original variables,

$$u_i = 1 + \frac{2}{p}\ln\left(\cosh\frac{1}{2}p\sqrt{\lambda}y\right). \tag{12}$$

We note that $u_i \to 1 - \frac{2}{p}\ln 2 + \sqrt{\lambda}y$ as $y \to \infty$.

To close the phase portraits, we will try to patch the two solutions together at a common point. That is, find a point $y = y_m$ such that

$$u_i(y_m) = u_0(y_m), \quad u_i'(y_m) = u_0'(y_m) \tag{13}$$

or, in detail,

$$\sqrt{\frac{\lambda + v}{v}} \cos\sqrt{v}(1 - y_m) = 1 + \frac{2}{p}\ln\left(\cosh\frac{1}{2}p\sqrt{\lambda}y_m\right) \tag{14.1}$$

$$\sqrt{\lambda + v} \sin\sqrt{v}(1 - y_m) = \sqrt{\lambda} \tanh\frac{1}{2}p\sqrt{\lambda}y_m \tag{14.2}$$

where higher order terms in y_m and p^{-1} have been neglected. Within terms of the order $(p\sqrt{\lambda})^{-1}$, the linear terms in y_m are eliminated by choosing

$$\sin\sqrt{v} = \frac{\sqrt{\lambda}}{\sqrt{\lambda + v}}. \tag{18}$$

Equation 18 could have been obtained directly by matching the slopes of inner and outer solutions, i.e., $u'_i(\infty) = u'_0(0)$.

It is clear that there are an infinity of solutions for v as a function of λ since the right-hand side of Equation 18 decreases monotonically from 1 towards 0 as v increases, whereas the left-hand side is periodic with repeated maxima of 1. Thus, there will be two solutions of Equation 18 for each maximum in the sine function. Since λ is expected to be large, the right-hand side decreases slowly with v, and the first intersection, which is also consistent with the desired phase portrait, will occur near the first maximum. It turns out that

$$\sqrt{v} = \frac{\pi}{2} - \varepsilon \text{ where } \varepsilon = 0(\lambda^{-1/2}) \tag{19}$$

and, consequently, the decay rate of the stress is given by

$$\alpha = \frac{\pi^2}{4}k. \tag{20}$$

Since Equation 19 shows that $v = 0(1)$, it would have been justified to ignore v in comparison with λ in Equation 9.

In principle, from the inverses of Equations 16 and 15.2, we could now go back to find y_m, which from Equation 15.2 must be $0(p\sqrt{\lambda})^{-1}$. But rather than doing that, we take the thickness of the boundary layer to be

$$\delta = 2/p\sqrt{\lambda} = \left(\frac{2mk}{(1 - m)\,aA^{1+m}}\right)^{1/2}$$

where the argument of cosh in Equation 12 is 1.

The amplitude A and band width δ may now be determined. The left-hand side of Equation 6 may be evaluated approximately as follows:

$$\begin{aligned}\int_0^1 u\,dy &= \int_0^\delta u_i\,dy + \int_\delta^1 u_0\,dy \\ &= \delta + v^{-1/2}\sqrt{1 + (\lambda/v)}\ [\sin\sqrt{v}\,(1 - \delta)] \\ &= v^{-1}\sqrt{\lambda}\,(1 + 0(\lambda^{-1/2}))\,. \end{aligned} \qquad (21)$$

Note that the value of the integral comes all from the outer solution for $\delta \ll 1$. Since the right hand side of Equation 6 is aA^m/kv after using Equation 8.3, we have $\sqrt{\lambda} = aA^m/k$, or with the aid of Equation 8.1,

$$A = \left(\frac{1 - m}{2}\frac{a}{mk}\right)^{1/(1-m)}. \qquad (22)$$

It is now easy to work out that

$$\delta = 1/A. \qquad (23)$$

Clearly, since $m \ll 1$, the condition that $\delta \ll 1$ and $A \gg 1$ reduces approximately to

$$\frac{k}{a} \ll \frac{1}{m}.$$

Also, since

$$\frac{2v}{\lambda p} = \frac{\pi^2}{4}\left\{\frac{2m}{1-m}\right\}^{\frac{1+m}{1-m}}\left\{\frac{k}{a}\right\}^{\frac{2}{1-m}},$$

the condition that was required to justify the inner solution, $2v/\lambda p \ll 1$, reduces approximately to $k/a \ll m^{-1/2}$, which is more stringent than the previous condition. However, the most stringent condition of all comes from the condition

$$\lambda = \left\{\frac{1-m}{2m}\right\}^{\frac{2m}{1-m}}\left\{\frac{a}{k}\right\}^{\frac{2}{1-m}} \gg 1,$$

which was required to obtain Equation 19. Since the first factor is 0(1) for small m, the approximate requirement is that $(k/a)^2 \ll 1$. From the nondimensionalization in Equation 2, it may be seen that the strong inequalities fail if the nominal applied strain rate, $\dot{\gamma}_0$, is too small. Finally, by back substitution we see that

$$x(\ln x)^{1/2} = \frac{2^{-\frac{m}{1-m}}}{\pi}\left(\frac{1-m}{m}\right)^{\frac{1+m}{2(1-m)}}\left(\frac{a}{k}\right)^{\frac{1}{1-m}},$$

which tends to infinity as m tends to zero (p tends to infinity), and thus justifies the assumptions associated with Equations 15, 16, and 17.

When Equations 22 and 23 are expressed in dimensional terms, it becomes clear that the maximum strain rate in the shear band and the thickness of the shear band depend only on the imposed velocity difference across the band, rather than on the imposed strain rate and slab width separately. Thus, converting Equation 22 back to dimensional quantities, we have

$$\dot{\gamma}_{max} = \dot{\gamma}_0 A = \dot{\gamma}_0 \left(\frac{1-m}{2m} \frac{aS_0}{\rho c} \frac{\rho c \dot{\gamma}_0 h^2}{k} \right)^{1/(1-m)}$$

$$= \left(\frac{1-m}{2m} \frac{-\partial\sigma_0/\partial\vartheta}{k} b^m \right)^{1/(1-m)} V_0^{2/(1-m)} . \qquad (24)$$

In the final form of Equation 24, the expression

$$a = \frac{-1}{S_0} \frac{\partial s}{\partial \vartheta} = \frac{-1}{S_0} \frac{\partial \sigma_0}{\partial \vartheta} (b\dot{\gamma}_0)^m$$

has been used, and $\partial\sigma_0/\partial\vartheta$ represents the rate of thermal softening under quasi-static conditions and ambient temperature. In the present model, $\sigma_0 = \kappa_0 (1 - a\vartheta)$, and the derivative is evaluated at $\vartheta = 0$. Similarly, the dimensional form of Equation 23 becomes

$$\delta = h/A = \left(\frac{1-m}{2m} \frac{-\partial\sigma_0/\partial\vartheta}{k} b^m \right)^{-1/(1-m)} V_0^{-\frac{1+m}{1-m}} . \qquad (25)$$

4. NUMERICAL EXAMPLE AND CONCLUSIONS

Wright and Walter (1987) used the following nondimensional data in their full finite element calculations with $\dot{\gamma}_0 = 500 s^{-1}$:

$$m = 0.0251, \quad k = 0.0022, \quad a = 0.104 \times (5 \times 10^6)^{0.0251}.$$

The softening coefficient, a, has been multiplied here by the factor $(b\dot{\gamma}_0)^m$ to account for the fact that Wright and Walter scaled stresses by κ_0, whereas stresses have been scaled by S_0 in this report. The data lead to the values A = 1,628 and $\log_{10} \delta = 3.212$, which appear to be extremely accurate when compared to Wright and Walter's Figure 7 (see Figure 2 of this report). Note that the two curves differ only slightly and only at the top; the estimate for δ lies at the point where the strain rate has fallen to approximately 40% of its maximum value.

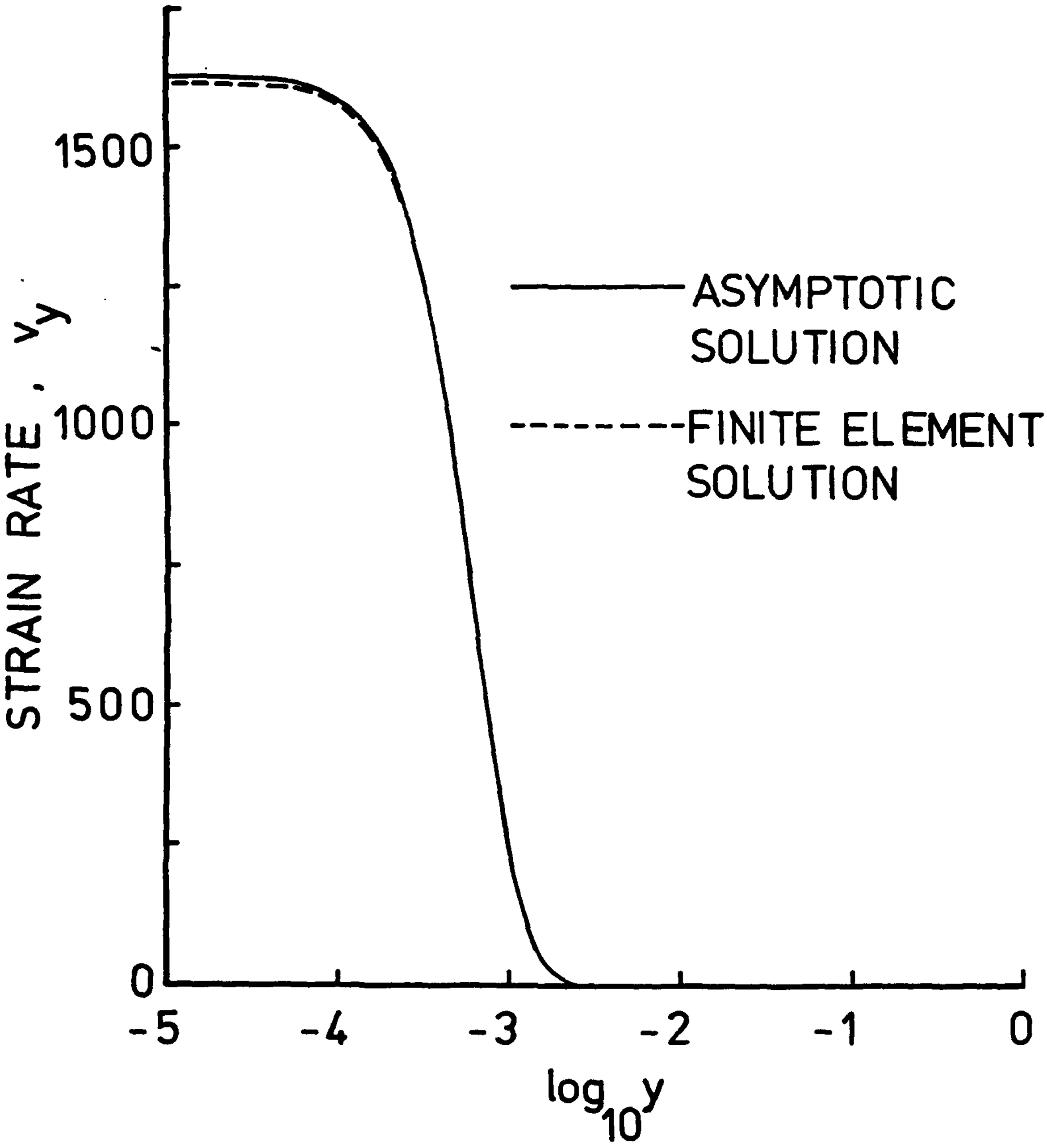

Figure 2. Comparison of Present Asymptotic Solution With Finite Element Solution Due to Wright and Walter (1987).

Equations 24 and 25 give the basic scaling laws for the intensity and width of the strain rate profile. For $m \ll 1$, as in metals, neither $\dot{\gamma}_{max}$ nor the dimensional value of δ is sensitive to the exact value of b. As expected, the maximum strain rate increases with the rate of softening, but decreases with strain rate sensitivity and thermal conductivity, and the width of the strain rate profile varies in the opposite sense. As has already been noted, both quantities depend only on v_0, and not on $\dot{\gamma}_0$ and h separately. It is interesting to note that neither quantity depends on either the density or the heat capacity, which is a consequence of the nearly steady feature of fully formed bands.

One last consequence of Equations 24 and 25, which may have some experimental significance even though it has been obtained with a special flow law, is that the product of the maximum strain rate and the band width is equal to the imposed velocity

$$\delta\dot{\gamma}_{max} = v_0 \,. \tag{26}$$

The width δ as obtained in this analysis is the distance from the center of the band at which the strain rate is less than the maximum value by a factor of

$$\left(1 + \frac{.9}{p}\right)^{1/m} \approx e^{.9/(1-m)},$$

(or about 2.5), but from there on the strain rate decreases so rapidly that this estimate of width should be as good as any.

In an experimental sense the "width" of a shear band is often associated with the width of a "white etching band," which in the older literature has often been referred to as a "transformed band," implying that a metallurgical transformation has occurred that causes the material in the band to etch in a manner different from the surrounding material. If that "transformation" is associated only with the extreme straining in the fully formed band, leading perhaps to ultra fine grain refinement with little or no recrystalization, as recent work suggests for 4340 steels (e.g., Beatty et al. 1990*), then estimates of the kind given in Equations 25 and 26 should be accurate and useful for "transformed" bands, as well as for the simpler "deformed" bands, where localization has occurred without a change in etching behavior. On the other hand, metallurgical transformations have not yet been included in any theoretical treatment and, in any case, may be associated with the thermal profile, which is much wider than the strain rate profile. Therefore, a more comprehensive estimate of "band width" for cases with true transformations remains lacking.

As a final comment, the reader is reminded that the results in this paper are specific for the assumed flow law in Equation 3.3, which is intended to describe a perfectly plastic material with linear thermal softening and power law rate hardening. In fact, the separation of variables that is shown in Equation 5 only occurs exactly in the case of linear softening. Nevertheless, the methods and results shown here are broadly suggestive for more general cases, for example, when the softening rate varies slowly with temperature, or when work hardening nears saturation.

---

* The authors are grateful to a reviewer for calling this reference to their attention.

INTENTIONALLY LEFT BLANK.

5. REFERENCES

Beatty, J. H., L. W. Meyer, M. A. Meyers, and S. Nemat-Nassar. MTL TR90-54, U.S. Army Materials Technology Laboratory, Watertown, MA, 1990.

Walter, J. W. "Numerical Experiments on Adiabatic Shear Bands." International Journal of Plasticity, to appear in 1992.

Wright, T. W., and J. W. Walter. Journal of the Mechanics and Physics of Solids, vol. 35, no. 701, 1987.

INTENTIONALLY LEFT BLANK.

No. of Copies	Organization
2	Administrator Defense Technical Info Center ATTN: DTIC-DDA Cameron Station Alexandria, VA 22304-6145
1	Commander U.S. Army Materiel Command ATTN: AMCAM 5001 Eisenhower Ave. Alexandria, VA 22333-0001
1	Commander U.S. Army Laboratory Command ATTN: AMSLC-DL 2800 Powder Mill Rd. Adelphi, MD 20783-1145
2	Commander U.S. Army Armament Research, Development, and Engineering Center ATTN: SMCAR-IMI-I Picatinny Arsenal, NJ 07806-5000
2	Commander U.S. Army Armament Research, Development, and Engineering Center ATTN: SMCAR-TDC Picatinny Arsenal, NJ 07806-5000
1	Director Benet Weapons Laboratory U.S. Army Armament Research, Development, and Engineering Center ATTN: SMCAR-CCB-TL Watervliet, NY 12189-4050
(Unclass. only) 1	Commander U.S. Army Rock Island Arsenal ATTN: SMCRI-TL/Technical Library Rock Island, IL 61299-5000
1	Director U.S. Army Aviation Research and Technology Activity ATTN: SAVRT-R (Library) M/S 219-3 Ames Research Center Moffett Field, CA 94035-1000
1	Commander U.S. Army Missile Command ATTN: AMSMI-RD-CS-R (DOC) Redstone Arsenal, AL 35898-5010

No. of Copies	Organization
1	Commander U.S. Army Tank-Automotive Command ATTN: ASQNC-TAC-DIT (Technical Information Center) Warren, MI 48397-5000
1	Director U.S. Army TRADOC Analysis Command ATTN: ATRC-WSR White Sands Missile Range, NM 88002-5502
1	Commandant U.S. Army Field Artillery School ATTN: ATSF-CSI Ft. Sill, OK 73503-5000
(Class. only) 1	Commandant U.S. Army Infantry School ATTN: ATSH-CD (Security Mgr.) Fort Benning, GA 31905-5660
(Unclass. only) 1	Commandant U.S. Army Infantry School ATTN: ATSH-CD-CSO-OR Fort Benning, GA 31905-5660
1	WL/MNOI Eglin AFB, FL 32542-5000
	<u>Aberdeen Proving Ground</u>
2	Dir, USAMSAA ATTN: AMXSY-D AMXSY-MP, H. Cohen
1	Cdr, USATECOM ATTN: AMSTE-TC
3	Cdr, CRDEC, AMCCOM ATTN: SMCCR-RSP-A SMCCR-MU SMCCR-MSI
1	Dir, VLAMO ATTN: AMSLC-VL-D
10	Dir, USABRL ATTN: SLCBR-DD-T

No. of Copies	Organization
1	Director U.S. Army Research Office ATTN: J. Chandra P.O. Box 12211 Research Triangle Park, NC 27709-2211
1	Director U.S. Army Research Office ATTN: I. Iyer P.O. Box 12211 Research Triangle Park, NC 27709-2211
1	Director U.S. Army Research Office ATTN: J. Wu P.O. Box 12211 Research Triangle Park, NC 27709-2211
3	Director U.S. Army Materials Technology Laboratory ATTN: SLCMT-MRD, T. Weerasooriya S. Chou J. Dandekar Watertown, MA 21720-0001
1	Commander U.S. Army Tank-Automotive Command ATTN: AMSTA-RSS Warren, MI 48397-5000
1	U.S. Naval Academy Department of Mathematics ATTN: R. Malek-Madani Annapolis, MD 21402
1	Air Force Armament Laboratory ATTN: J. Foster Eglin AFB, FL 32542-5438
1	Air Force Wright Aeronautical Laboratories Air Force Systems Command Materials Laboratory ATTN: T. Nicholas Wright-Patterson AFB, OH 45433

No. of Copies	Organization
3	Sandia National Laboratories ATTN: L. Davison W. Herrmann P. Chen P.O. Box 5800 Albuquerque, NM 87285-5800
1	Sandia National Laboratories ATTN: S. Passman P.O. Box 5800 Albuquerque, NM 87285-5800
1	Sandia National Laboratories ATTN: M. Forrestal P.O. Box 5800 Albuquerque, NM 87285-5800
1	Sandia National Laboratories ATTN: D. Bammann Livermore, CA 94550
1	National Institute of Science and Technology ATTN: T. Burns Technology Building, Room A151 Gaithersburg, MD 20899
1	University of Missouri-Rolla Dept. of Mechanical and Aerospace Engineering ATTN: R. Batra Rolla, MO 65401-0249
1	California Institute of Technology Division of Engineering and Applied Science ATTN: J. Knowles Pasadena, CA 91102
1	Massachusetts Institute of Technology Dept. of Mechanical Engineering ATTN: L. Anand Cambridge, MA 02139
2	Rennselaer Polytechnic Institute Department of Mechanical Engineering ATTN: E. Lee E. Krempl Troy, NY 12181

No. of Copies	Organization
1	Rennselaer Polytechnic Institute Dept. of Computer Science ATTN: J. Flaherty Troy, NY 12181
1	Brown University Division of Engineering ATTN: R. Clifton Providence, RI 02912
1	Brown University Division of Engineering ATTN: J. Duffy Providence, RI 02912
1	Brown University Division of Engineering ATTN: B. Freund Providence, RI 02912
1	Brown University Division of Engineering ATTN:A Needleman Providence, RI 02912
1	Brown University Division of Applied Mathematics ATTN: C. Dafermos Providence, RI 02912
1	Carnegie-Mellon University Dept. of Mathematics ATTN: D. Owen Pittsburg, PA 15213
1	Carnegie-Mellon University Dept. of Mathematics ATTN: M. Gurtin Pittsburg, PA 15213
1	Cornell University Dept. of Theoretical and Applied Mechanics ATTN: J. Jenkins Ithaca, NY 14850
1	Cornell University Dept. of Theoretical and Applied Mechanics ATTN: P. Rosakis Ithaca, NY 14850

No. of Copies	Organization
1	Cornell University Dept. of Theoretical and Applied Mechanics ATTN: W. Sachse Ithaca, NY 14850
1	Cornell University Dept. of Theoretical and Applied Mechanics ATTN: T. Healey Ithaca, NY 14850
1	Cornell University Dept. of Theoretical and Applied Mechanics ATTN: A. Zehnder Ithaca, NY 14850
1	Harvard University Division of Engineering and Applied Physics ATTN: J. Rice Cambridge, MA 02138
1	Harvard University Division of Engineering and Applied Physics ATTN: J. Hutchinson Cambridge, MA 02138
1	Lehigh University Center for the Application of Mathematics ATTN: E. Varley Bethlehem, PA 18015
1	North Carolina State University Dept. of Civil Engineering ATTN: Y. Horie Raleigh, NC 27607
1	Rice University Dept of Mathematical Sciences ATTN: C. C. Wang P.O. Box 1892 Houston, TX 77001
1	The Johns Hopkins University Dept. of Mechanical Engineering Latrobe Hall ATTN: W. Sharp 34th and Charles Streets Baltimore, MD 21218

No. of Copies	Organization
1	The Johns Hopkins University Dept. of Mechanical Engineering Latrobe Hall ATTN: G. Bao 34th and Charles Streets Baltimore, MD 21218
1	The Johns Hopkins University Dept. of Mechanical Engineering Latrobe Hall ATTN: K. T. Ramesh 34th and Charles Streets Baltimore, MD 21218
1	The Johns Hopkins University Dept. of Mechanical Engineering Latrobe Hall ATTN: A. Douglas 34th and Charles Streets Baltimore, MD 21218
1	University of California at Santa Barbara Dept of Materials Science ATTN: A. Evans Santa Barbara, CA 93106
1	University of California at San Diego Dept. of Applied Mechanics and Engineering Sciences ATTN: S. Nemat-Nasser La Jolla, CA 92093
1	University of California at San Diego Dept. of Applied Mechanics and Engineering Sciences ATTN: M. Meyers La Jolla, CA 92093
1	University of California at San Diego Dept. of Applied Mechanics and Engineering Sciences ATTN: X. Markenscoff La Jolla, CA 92093

No. of Copies	Organization
1	University of California at San Diego Dept. of Applied Mechanics and Engineering Sciences ATTN: A. Hoger La Jolla, CA 92093
1	University of California at San Diego Dept. of Applied Mechanics and Engineering Sciences ATTN: R. Asaro La Jolla, CA 92093
1	Northwestern University Dept. of Applied Mathematics ATTN: W. Olmstead Evanston, IL 60201
1	University of Florida Dept. of Engineering Science and Mechanics ATTN: L. Malvern Gainesville, FL 32601
1	University of Florida Dept. of Engineering Science and Mechanics ATTN: D. Drucker Gainesville, FL 32601
1	University of Florida Dept. of Engineering Science and Mechanics ATTN: M. Eisenberg Gainesville, FL 32601
1	University of Houston Dept. of Mechanical Engineering ATTN: L. Wheeler Houston, TX 77004
1	University of Illinois Dept. of Theoretical and Applied Mechanics ATTN: D. Carlson Urbana, IL 61801

No. of Copies	Organization
1	University of Illinois at Chicago Circle Dept. of Engineering, Mechanics, and Metallurgy ATTN: T. Ting P.O. Box 4348 Chicago, IL 60680
1	University of Kentucky Dept. of Engineering Mechanics ATTN: O. Dillon, Jr. Lexington, KY 40506
1	University of Maryland Dept. of Mathematics ATTN: S. Antman College Park, MD 20742
1	University of Maryland Dept. of Mathematics ATTN: T. Liu College Park, MD 20742
1	University of Minnesota Dept. of Aerospace Engineering and Mechanics ATTN: R. Fosdick 110 Union Street SE Minneapolis, MN 55455
1	University of Minnesota Dept. of Aerospace Engineering and Mechanics ATTN: R. James 110 Union Street SE Minneapolis, MN 55455
1	University of Oklahoma School of Aerospace, Mechanical and Nuclear Engineering ATTN: C. Bert Norman, OK 73019
1	University of Texas Dept. of Engineering Mechanics ATTN: J. Oden Austin, TX 78712

No. of Copies	Organization
1	University of Washington Dept. of Aeronautics and Astronautics ATTN: I. Fife 206 Guggenheim Hall Seattle, WA 98195
1	University of Maryland Dept. of Mechanical Engineering ATTN: R. Armstrong College Park, MD 20742
1	University of Maryland Dept. of Mechanical Engineering ATTN: J. Dally College Park, MD 20742
1	University of Wyoming Dept. of Mathematics ATTN: R. Ewing P.O. Box 3036 University Station Laramie, WY 82070
1	Washington State University Mechanical and Materials Engineering ATTN: H. M. Zbib Pullman, WA 99164
1	Yale University Dept. of Mechanical Engineering ATTN: E. Onat 400 Temple Street New Haven, CT 96520
1	Southwest Research Institute Department of Mechanical Sciences ATTN: U. Lindholm 8500 Culebra Road San Antonio, TX 02912
1	Southwest Research Institute Department of Mechanical Sciences ATTN: C. Anderson 8500 Culebra Road San Antonio, TX 02912

No. of Copies	Organization
1	Southwest Research Institute Department of Mechanical Sciences ATTN: J. Lankford 8500 Culebra Road San Antonio, TX 02912
1	The Johns Hopkins University Materials Science and Engineering ATTN: R. E. Green 102 Maryland Hall Baltimore, MD 21218
1	University of Nebraska Engineering Mechanics ATTN: M. Beatty 212 Bancroft Hall Lincoln, NE 68588
1	Oklah..na State University ATTN: R. M. Bowen 101 Whitehurst Hall Stillwater, OK 74078
1	University of Maryland Baltimore County Mechanical Engineering ATTN: A. Khan Baltimore, MD 21228
1	University of Wisconsin Dept. of Mathematics ATTN: A. Tzavaras Madison, WI 53706
1	California Institute of Technology ATTN: G. Ravichandran Mail Code 105-50 Pasadena, CA 91125
1	State University of New York at Stony Brook Applied Mathematics and Statistics P138A Mathematics ATTN: J. Glimm Stony Brook, NY 11794

No. of Copies	Organization
1	University of Virginia Dept. of Applied Mathematics ATTN: C. O. Horgan Thornton Hall Charlottesville, VA 22903
1	Drexel University Dept. of Materials Engineering ATTN: H. C. Rogers Philadelphia, PA 18104
1	SRI International ATTN: D. Curran 333 Ravenswood Avenue Menlo Park, CA 94025
1	SRI International ATTN: R. Shockey 333 Ravenswood Avenue Menlo Park, CA 94025
1	SRI International ATTN: L. Seaman 333 Ravenswood Avenue Menlo Park, CA 94025

USER EVALUATION SHEET/CHANGE OF ADDRESS

This Laboratory undertakes a continuing effort to improve the quality of the reports it publishes. Your comments/answers to the items/questions below will aid us in our efforts.

1. BRL Report Number BRL-MR-3993 Date of Report August 1992

2. Date Report Received ____________________

3. Does this report satisfy a need? (Comment on purpose, related project, or other area of interest for which the report will be used.) ____________________

4. Specifically, how is the report being used? (Information source, design data, procedure, source of ideas, etc.) ____________________

5. Has the information in this report led to any quantitative savings as far as man-hours or dollars saved, operating costs avoided, or efficiencies achieved, etc? If so, please elaborate. ____________________

6. General Comments. What do you think should be changed to improve future reports? (Indicate changes to organization, technical content, format, etc.) ____________________

CURRENT ADDRESS

Name

Organization

Address

City, State, Zip Code

7. If indicating a Change of Address or Address Correction, please provide the New or Correct Address in Block 6 above and the Old or Incorrect address below.

OLD ADDRESS

Name

Organization

Address

City, State, Zip Code

(Remove this sheet, fold as indicated, staple or tape closed, and mail.)

DEPARTMENT OF THE ARMY
Director
U.S. Army Ballistic Research Laboratory
ATTN: SLCBR-DD-T
Aberdeen Proving Ground, MD 21005-5066

OFFICIAL BUSINESS

BUSINESS REPLY MAIL
FIRST CLASS PERMIT No 0001, APG, MD

Postage will be paid by addressee.

Director
U.S. Army Ballistic Research Laboratory
ATTN: SLCBR-DD-T
Aberdeen Proving Ground, MD 21005-5066

NO POSTAGE
NECESSARY
IF MAILED
IN THE
UNITED STATES